Transactions on Electrical and Electronic Materials
https://doi.org/10.1007/s42341-024-00560-1

Online ISSN 2092-7592
Print ISSN 1229-7607

REGULAR PAPER

Design and Investigation of Gate Overlap Step Shape Double Gate (SSDG) TFET for Photosensing Applications

Nidhish Tiwari[1] · Rajesh Saha[2] · Bharat Choudhary[1]

Received: 3 May 2024 / Revised: 19 June 2024 / Accepted: 17 July 2024
© The Korean Institute of Electrical and Electronic Material Engineers 2024

Abstract

This work examines the optical properties of Gate Overlap Step Shape Double Gate Tunnel Field Effect Transistor (GO-SSDG-TFET) based photosensor in the visible spectrum range at wavelengths ($\lambda = 300$–700 nm). We have presented a comparative study of Ge source GO-SSDG-TFET with the conventional Si source TFET at constant intensity (I) of 0.7 W/cm^2 for three distinct $\lambda = 300$, 500, and 700 nm. We have extracted the drain current, electron density, and energy band diagram for these photosensor at different λ. Moreover, the optical parameters like sensitivity (S_n), Signal to Noise Ratio (SNR), responsivity (R) and quantum efficiency (η) are reported for the considered photo sensors. Both the photosensor reports excellent optical features because of its huge absorption and emission rates, which is a result of the high incoming optical energy (E_g) at $\lambda = 300$ nm. Moreover, the optical properties of Ge-GO-SSDG-TFET is superior than Si based photosensor. The obtained values of sensitivity, SNR, and responsivity are 86.2, 72.5 dB, and 0.71 A/Watt, respectively, at $\lambda = 300$ nm for Ge-GO-SSDG-TFET. Finally, a tabular summary of optical parameters between a suggested TFET-based photosensor with the photosensor mentioned in the literature is presented.

Keywords Photosensor · Responsivity · Spectral sensitivity · TFET

1 Introduction

Numerous FET-based optical devices with outstanding optical properties at tuneable wavelengths have been published in the literature in recent years [1–3]. A device's optical performance is affected by a variety of elements, including the wavelength of incident light, light's emission rate, and the absorption coefficient of a sensitive substance. These factors have significant effect on the optical behaviour of FETs. At room temperature, the subthreshold swing (SS) of FET devices is restricted to 60 mV/dec. [4]. Tunnel field effect transistors (TFETs) respond quickly to visible spectrum of light because they have SS value which does not exceed 60 mV/decade and can switch ON and OFF quickly [5, 6]. Furthermore, TFETs are better suited for low power applications since they may operate at a lower voltage than traditional FET devices. Owing to its advantages over MOSFET, it has gained recognition as a better substitute in recent times. However, the low ON and ambipolar current of TFETs limits the possible applications in a number of ways [7, 8]. Numerous technologies are being used to address these identified vulnerabilities. Lowering the dopant concentration in the drain region [7], adding a high-k dielectric oxide layer [9] next to boost the rate of tunnelling to the source side, and introducing an area of horizontal pockets [10] in the source are some intriguing techniques for a greater range of uses, such photosensors. These modifications to the standard TFET's design aim to lessen these innate shortcomings and make it suitable for a greater variety of uses, including energy harvesting, photosensors, biosensors, and gas sensors [11–14].

Researchers have employed a variety of techniques in literature to enhance the performance of TFETs, including dual gate oxide [9], pocket insertion [15], and the addition

✉ Rajesh Saha
rajeshsaha93@gmail.com

Nidhish Tiwari
nidhishtiwari@gmail.com

Bharat Choudhary
bharat.ece@mnit.ac.in

[1] Department of Electronics and Communication Engineering, Malaviya National Institute of Technology Jaipur, Jaipur, Rajasthan 302017, India

[2] Department of Electronics and Communication Engineering, NIT Silchar, Silchar, Assam, India

Published online: 03 August 2024

of a high-k spacer [16]. It is commonly recognized that these changes increase the I_{ON}, decrease the I_{AMB}, and enhanced controllability of TFET over the channel. TFET is a crucial component of neuromorphic applications because of its fast-switching speed and low power consumption [17, 18]. The Gate Overlap Step Shape Double Gate TFET (SSDG-TFET) is a developing structure of TFET that provides considerable tunnelling across the source and channel regimes due to the extension of the source into the channel area [19]. This expanded source area in the channel region provides a higher ON current and better controllability. The SSDG-TFET is regarded as a crucial TFET because of its improved electrical characteristics, which have been documented in the literature [20]. In SSDG-TFET, switching occurs more efficiently and drain current increases as the P^+ source moves into the channel area. In this TFET design, a pair of distinct gate oxide layers promotes carrier conduction of charge carriers with minimal leakage current. Reduced power consumption is made possible by TFETs' low operational gate voltage (V_{gs}).

Based on the carriers' photon absorption and electron emission, an optical study of the SSDG-TFET photodetector functioning in visible light is covered in this work by altering wavelength (λ) from 300 to 700 nm. Moreover, TFET-driven optical characteristics under light conditions yields properties including SNR, quantum efficiency, sensitivity, and responsivity are studied. Both the characteristics of the material and the light's wavelength impinge on the sensitive areas affect these optical features. Lastly, a comparison table that contrasts the suggested photodetector's optical behaviour with published FET-based photodiodes has been presented.

The various section of this paper are: the device construction and simulation methods are presented in Sect. 2, the findings and discussion of the optical investigations at different wavelengths are summarized in Sect. 3, and this work is concluded in Sect. 4.

2 Device Structure and Simulation Methodology

The 2D view of Gate Overlap Step Shape Double Gate TFET (GO-SSDG-TFET) with Si and Ge as the source material are shown in Fig. 1a, b, respectively. In GO-Ge-SSDG-TFET, the source is Ge material with channel and drain regions are made of Silicon. However, in GO-Si-SSDG-TFET, all source, channel, and drain regions are made of Silicon. SiO_2 is used as gate dielectric for both the structures and poly silicon as gate material. As shown in Fig. 1, the GO-SSDG-TFET features a gate overlap the spans of the sections. The channel has a noteworthy quantity of line and point tunnelling, which promotes tunnelling in both vertical and horizontal directions.

The various dimensions are: length of top gate ($L_1 = 20$ nm, $L_2 = 15$ nm), length of bottom gate ($L_3 = 15$ nm, $L_4 = 15$ nm), length of overlap region ($L_O = 5$ nm), oxide thickness near source region ($t_{ox} = 2$ nm), oxide thickness near drain region ($t_{oxd} = 6$ nm), thickness of Si body ($t_{Si} = 10$ nm), length of source/drain regions are equal ($L_s = L_d = 20$ nm). The p^+ source in SSDG-TFET contributes

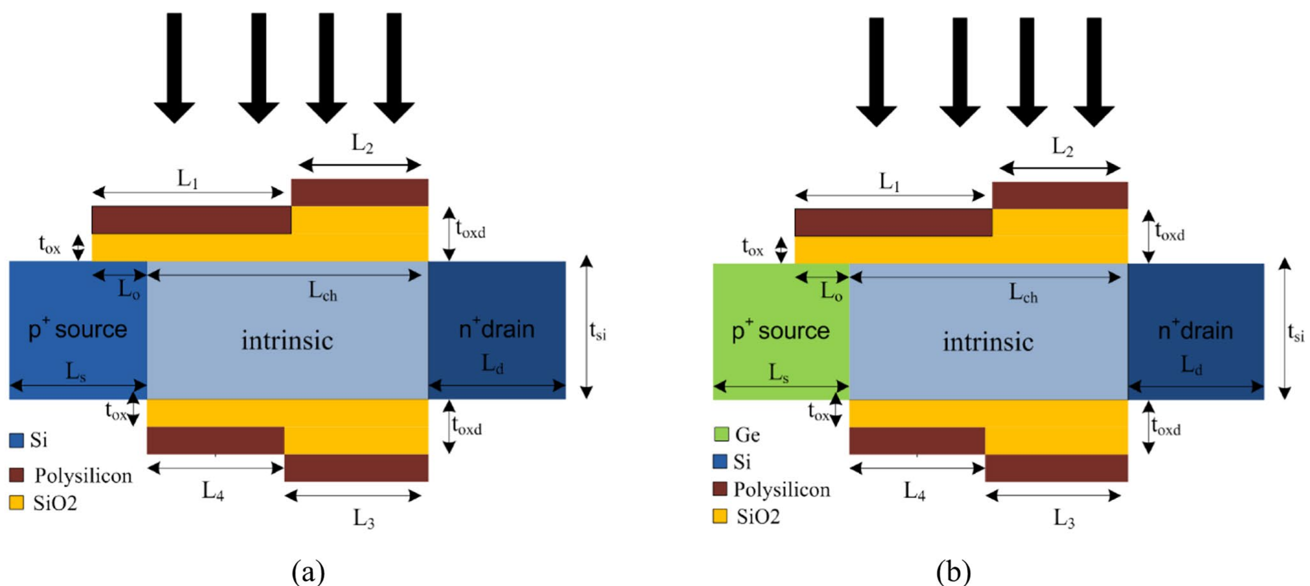

Fig. 1 2D view of **a** gate overlap step shape double gate TFET with Si source (GO-Si-SSDG-TFET) and **b** gate overlap step shape double gate TFET with Ge source (GO-Ge-SSDG-TFET)

to the tunnelling process with a doping concentration of 10^{20} cm^{-3}. Furthermore, the drain is composed of an n^+ type with a concentration of 10^{18} cm^{-3}, and the channel is built with lightly doped n type material having concentration of 10^{15} cm^{-3}. The work function of gate material is considered as 4.2 eV. Electron emission and photon absorption are the process that occurs along the metal gate region and activated when a certain wavelength of light contacts the photosensitive portion of the polysilicon metal gate.

Utilizing the Sentaurus TCAD tool, the optical characteristics of SSDG-TFETs are examined in the visible spectrum of light [21]. During the simulation, a non-local BTBT model is used to calculate the energy band gradient along the path. Since the source and drain regions are heavily doped, the band gap mechanism is represented by a band gap narrowing model. The generation-recombination process of the charge carriers is addressed by the Shockley Heal recombination model. The Fermi model is enabled due to heavily doped source and drain areas in the simulator. A calibration of experimental data with the simulator is performed to achieve the realistic data from the simulator. The various indirect tunneling coefficients are: $A = 3.29 \times 10^{15}$ cm^{-3} s^{-1}, $B = 23.8 \times 10^6$ V cm^{-1} for Si and $A = 1.67 \times 10^{15}$ cm^{-3} s^{-1}, $B = 6.55 \times 10^6$ V cm^{-1} for Ge are assumed for calibration [22]. A close matching is observed between the experimental and simulated data as shown in Fig. 2 [23].

In order to extract the optical characteristics of SSDG TFETs, we have defined the incident light wavelength and illumination intensity in TCAD simulator. The gate region for this TFET is assumed as illumination window through which optical operation take place and this window is considered in the simulator. Moreover, the incidence angle of light is defined in physics section. The 0° of incidence angle indicates light is normally incident and 90° represents that light is along the illuminated region [21]. We have considered the range of incident light wavelength ($\lambda = 0.3$–0.7) µm at constant illumination Intensity 0.8 W/cm^2.

Figure 3 represents the optical generation rate of Ge based photosensor at different values of λ at intensity of $I = 0.8$ W/cm^2. It is seen that optical generation rate is reduced as λ is changed from 300 to 700 nm and this is due to inverse relationship between optical energy and λ ($E_g = hc/\lambda$, where, h is Plank's constant and c is velocity of light).

Additionally, Fig. 4a, b represents the energy bands for the Ge SSDG TFET photodetector at both the states of light and dark, respectively, at various wavelengths. Likewise, the corresponding energy bands for Si SSDG-TFET photodetector is portrayed in Fig. 5a, b, at dark and light states, respectively. The electrons generated by photo production begin to allow current to flow when the gate voltage (V_{gs}) is applied, while holes begin to accumulate at the gate's oxide layer area. These conditions of charge separation cause the fermi equilibrium energy levels (E_{fn} and E_{fp}) to start fluctuating, creating within the photosensitive gate area, a potential of TFETs that is referred to as the photo voltage (V_{OP}). Since photo conduction doesn't happen in the device's lit area while it's dark, it can be shown in Figs. 4a and 5a, there is a collinear relationship between the fermi energy levels (E_{fn} and E_{fp}). Figure 5b displays the energy band diagram under illumination conditions. It is evident that the difference between the fermi energy levels (E_{fn} and E_{fp}) reduces as wavelength increases from 300 to 700 nm. The amplitude of the optical photovoltaic (V_{OP}) diminishes as wavelength increases because there are fewer electrons emitted at the gate sensitive area due to a decrease in input light energy (E_g).

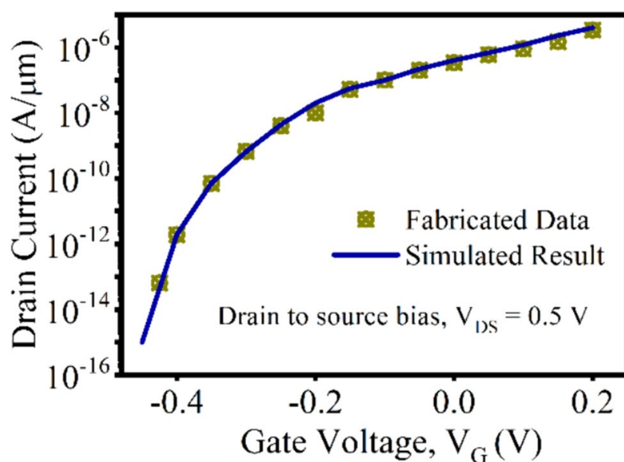

Fig. 2 Calibration of TCAD model with experimental data [23]

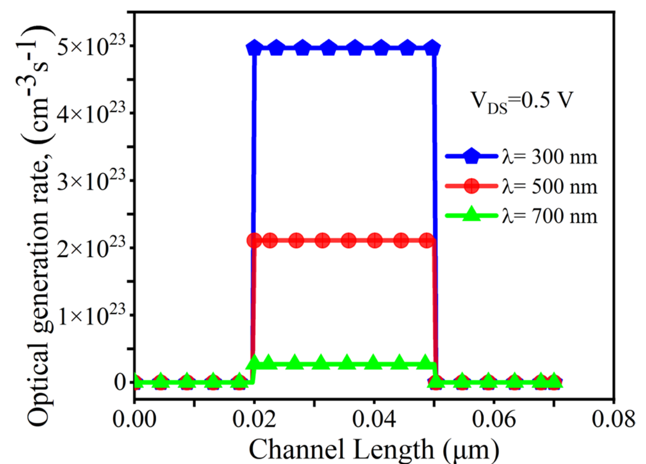

Fig. 3 Optical generation rate of Ge based GO-SSDG-TFET photosensor at different λ

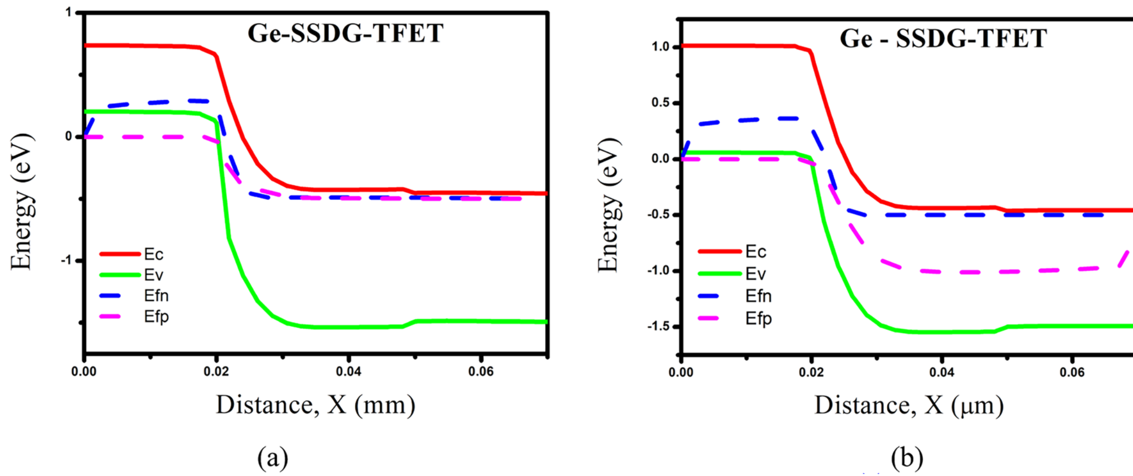

Fig. 4 Energy band diagram of Ge-SSDG-TFET based photodiode at the states of **a** dark and **b** light

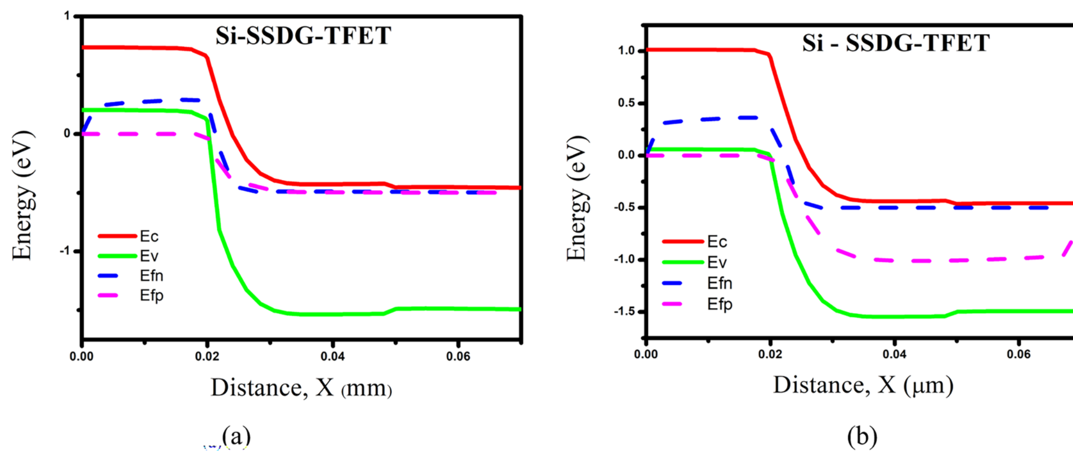

Fig. 5 Energy band diagram of Si-SSDG-TFET based photodiode at the states of **a** dark and **b** light

3 Results and Discussion

Figure 6 shows the transfer characteristic of Ge SSG-TFET-based photodiode's at three different visible spectrum wavelengths (λ = 300, 500, and 700 nm). It is seen that the fluctuation in drain current is larger, when the situation is lighted at extremely low V_{GS}. Moreover, when wavelength rises, the difference between the light and dark currents decreases. This is due to the fact that the emission and absorption processes also have a significant influence at low gate voltages and the gate electric field is also very tiny. The gadget becomes less sensitive as the voltage gradient grows because the gate exerts a greater influence on the channel.

Figure 7 shows transfer curve of Si SSDG-TFET photodiode at λ = 300, 500, and 700 nm at dark and light states. It is seen that under illumination state, the drain current

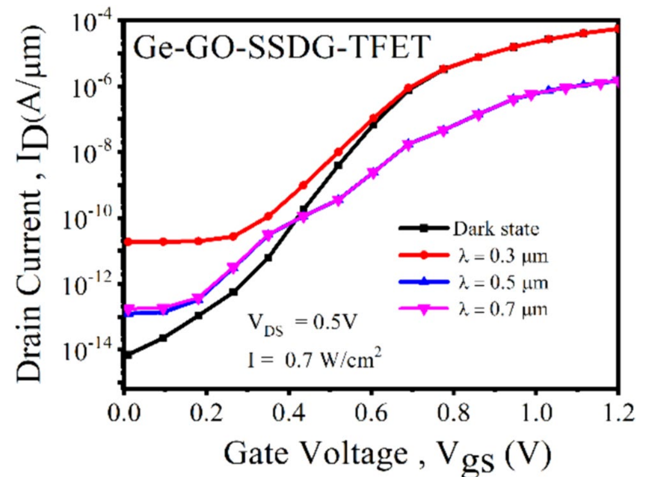

Fig. 6 I_d versus V_{gs} of Ge SSDG-TFET based photodiode at the state of dark and light for λ = 300, 500, and 700 nm

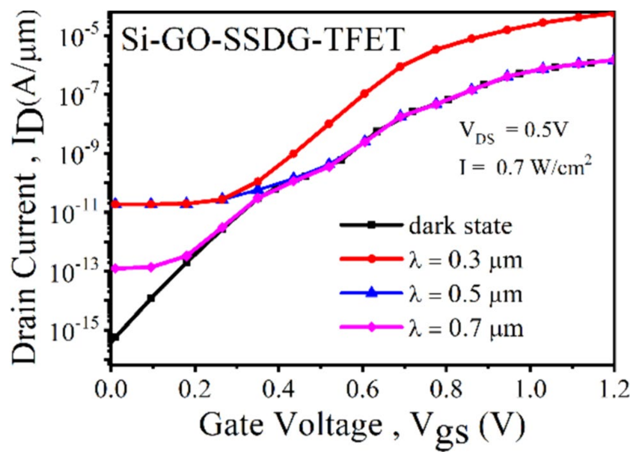

Fig. 7 I_d versus V_{gs} of Si SSDG-TFET based photodiode at the state of dark and light for λ = 300, 500, and 700 nm

degrades by significant amount at low gate bias than dark state current and this difference is negligible at high gate bias. The root cause of it the absorption rate is significantly decreases as λ is changed from 300 to 700 nm.

The electron density for Si and Ge GO-SSDG-TFET photosensor under both light and dark conditions are shown in Fig. 8. The electron density indicates the amount of charge carriers are present in a given volume, and large number of carriers indicates a higher drain current. It is seen from Fig. 8a, c that the electron density distribution is uniform under the dark state. However, an increased electron density at the channel region is perceived when exposed to light as shown in Fig. 8b, d. When light is injected across the photosensitive part of the device, this elevation in electron density implies an improvement in the optically generated absorption rate.

The several optical metrics, including Spectral Sensitivity (S_n), Signal to Noise Ratio (SNR), Responsivity (R), and Quantum Efficiency (Ƞ) are used to assess the influence of light on the SSDG-TFET based photodetectors. The various material qualities are used to determine the photon absorption and electron emission rates. As a result, the rate of generation can be expressed as [24–26]:

$$G_R = \alpha I_o \frac{h}{c\lambda}\left(1 - T_1\right)\left(1 - T_2\right)\left(1 - T_3\right) \quad (1)$$

α is absorption coefficient, I_o is the light Intensity, the reflection coefficients at the air/gate material, gate oxide/gate material, and gate oxide/semiconductor are denoted by T_1, T_2, and T_3, respectively.

The spectral sensitivity (S_n) is the ratio of difference in drain current between light and dark current to the dark current. It can be mathematically expressed as [27]:

$$S_n = \left(I_{light} - I_{dark}\right)/I_{dark} \quad (2)$$

I_{light} and I_{dark} are drain current under illuminated and dark states, respectively.

Figure 9a represents the sensitivity (S_n) of these photodiodes at different λ. It is seen that Ge-GO-SSDG TFET has improved sensitivity than Si-GO-SSDG-TFET due to presence of low bandgap Ge material at source region. The Ge based SSDG TFET has S_n of 86.2, 30.6, and 16.4 at λ = 300, 500, and 700 nm, respectively. Moreover, the sensitivity drops as wavelength (λ) increases because there are less emissions of electrons from the surface.

The signal to noise ratio (SNR) represents the amount of noise present at the device when operating at light state and can be expressed as [11, 28]:

$$SNR = 20log\left(I_{light}/I_{dark}\right) \quad (3)$$

Figure 9b represents the comparison of SNR value between Si-GO-SSDG and Ge-GO-SSDG TFET at three different λ = 300, 500, and 700 nm. It is observed that Ge device has higher value of SNR than Si based TFET and the value of SNR is reduced with increase in λ due to decrease in recombination rate.

Another crucial optical parameter is the Responsivity (R), which is affected by the wavelength of incident light and a function of quantum efficiency. Responsivity can be expressed as [27, 28]:

$$R = I_{light} - I_{dark}/I_o A = \frac{\text{Generated Photocurrent(I)}}{\text{Incident Optical Power(P)}} = \frac{q\lambda\eta}{hc} \quad (4)$$

where I_o is the light intensity and A is the effective illumination area of the sensor.

The calculated R at different values of λ for both the devices is portrayed in Fig. 9c. The calculated R are 0.51, 0.71, and 0.1 at λ = 300, 500 and 700 nm, respectively. Figure 9c also illustrates that there is a discernible drop in the value of R when λ is increased from 300 to 700 nm.

The Quantum efficiency (η) is a crucial optical metric as it represents the proportion of electron–hole pairs generated to photons incident across the sensor surface. It is mathematically defined as [28]:

$$\eta = \frac{\text{No. electron hole pair generated}}{\text{No. of photons Incident}} \quad (5)$$

The η of these photodiodes are compared at three different wavelengths of visible spectrum as shown in Table 1. It is observed that the photo detector's generation rate is greater at λ = 300 nm than other wavelengths. This is due to enhanced absorption coefficient with increased incoming optical energy (E_g) at lower value of λ, which leads to increased value in Ƞ.

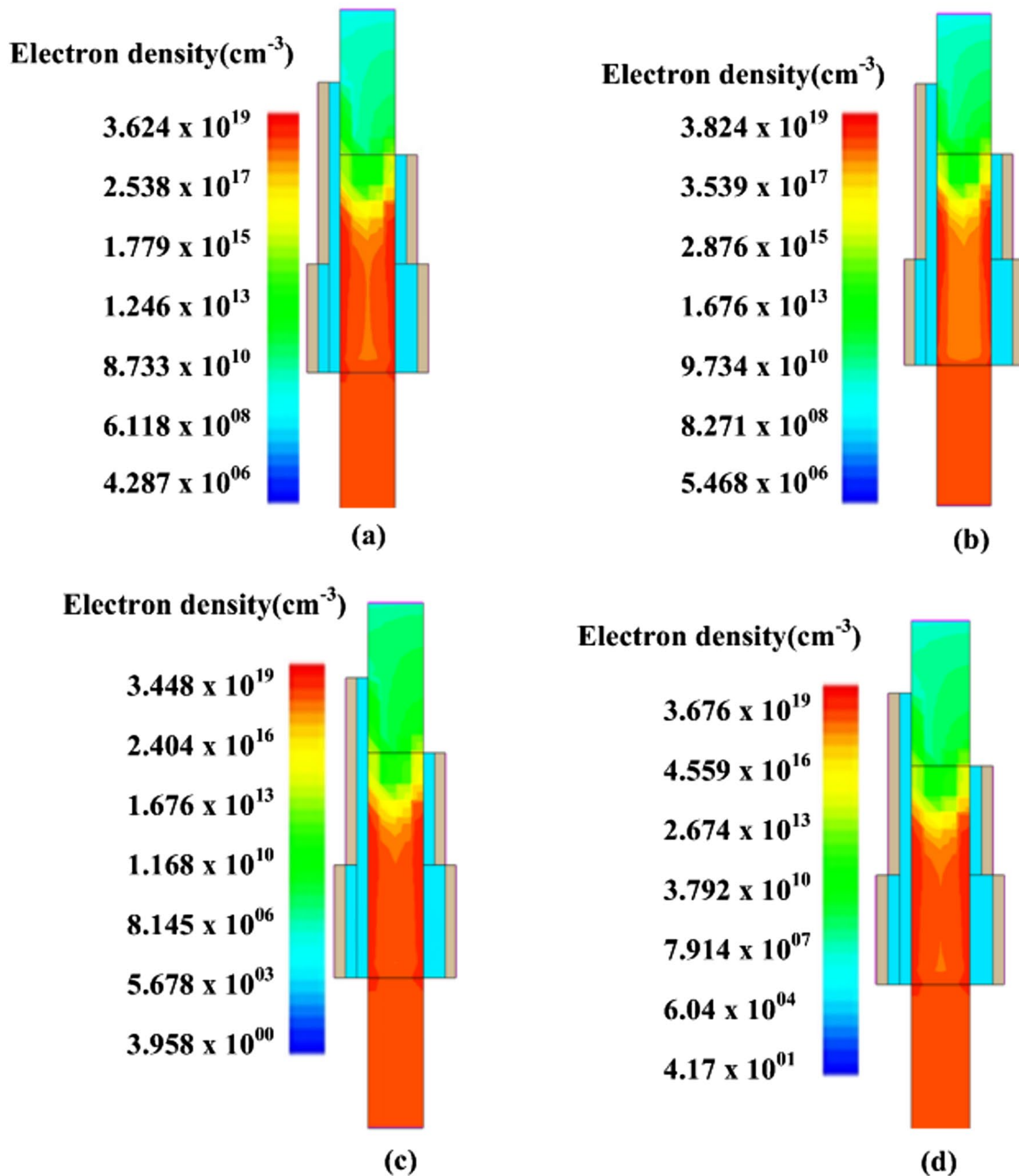

Fig. 8 Electron density **a**, **b** Ge-source GO-SSDG-TFET photosensor under dark and illumination states. **c**, **d** Si-GO-SSDG-TFET photosensor under dark and illumination states

Table 2 summarizes an overview of the SSDG-TFET photodiode's for Si and Ge source at various wavelengths. Here, BTBT rate, absorbed photon density, spectral density, SNR, and responsivity are reported for both the devices. We have examined the SSDG-TFET photosensors optical properties at three distinct wavelengths in order to assess the influence of wavelength in the visible spectrum. It is seen from Table 2 that SSDG-TFET photosensor performs admirably at lower λ values.

Table 3 summarizes a comparison of the optical properties for Ge-GO-SSDG TFET based photo sensor with those of photosensors found in the existing literature. The various structure, device dimensions, and doping specifications are not unique for the considered photodiode. It is seen from Table 3 that the Ge-GO-SSDG TFET based photodiode reports a maximum SNR of 72.5 dB, R value 0.71 A/watt,

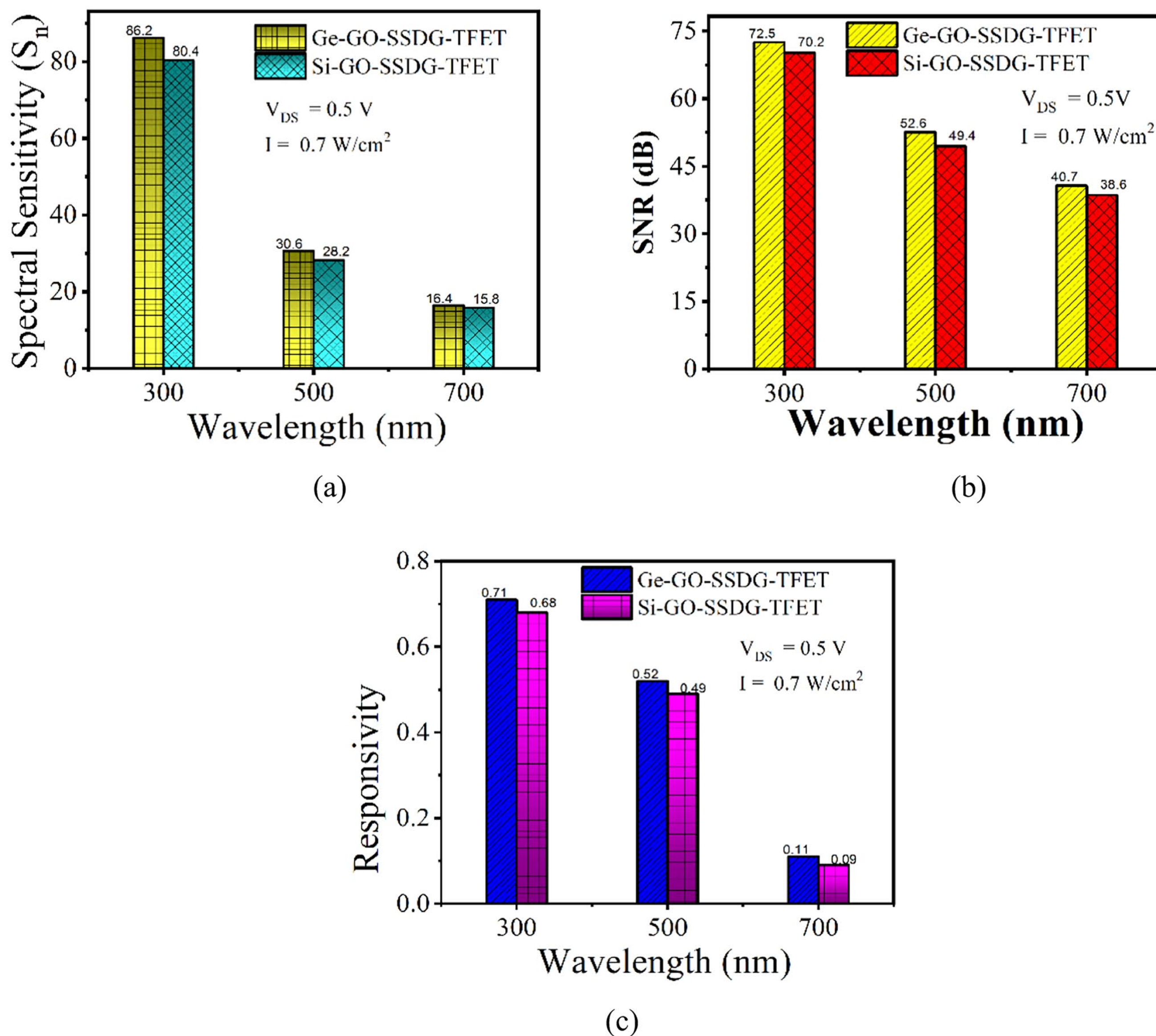

Fig. 9 Optical parameters of SSDG-TFET based photodiode's. **a** Spectral sensitivity, **b** SNR, and **c** responsivity at λ = 300, 500, and 700 nm

Table 1 Quantum efficiency of proposed Si and Ge GO-SSDG-TFET Photosensors at various λ

Parameters	λ = 300 nm		λ = 500 nm		λ = 700 nm	
	Ge	Si	Ge	Si	Ge	Si
Electron generation rate (cm^{-3} s^{-1})	8.94×10^{22}	6.81×10^{22}	3.13×10^{21}	5.34×10^{20}	7.96×10^{19}	9.87×10^{18}
Photon absorption rate (cm^{-3} s^{-1})	2.7×10^{23}	2.1×10^{23}	1.68×10^{22}	3.56×10^{21}	4.12×10^{21}	2.71×10^{20}
Quantum efficiency (η)	0.33	0.29	0.186	0.153	0.0193	0.0124

and S_n of 86.2 at incident λ = 300 nm. It is visualized from Table 3 that the Ge-GO-SSDG-TFET photosensor provides superior optical performance than existing TFET based photosensors.

Table 2 Comparative analysis of Si and Ge GO-SSDG-TFET photosensors at various λ

Wavelength (λ)	BTBT rate (cm^{-3} s^{-1})		Absorbed photon density (cm^{-3} s^{-1})		Spectral sensitivity		SNR (dB), $V_{GS}=0.1$ V		Responsivity (A/Watt)	
	Ge	Si	Ge	Si	Ge	Si	Ge	Si	Ge	Si
300 nm	10^{25}	10^{24}	2.7×10^{23}	2.1×10^{23}	86.2	80.4	72.5	70.2	0.71	0.68
500 nm	10^{24}	10^{23}	1.68×10^{22}	3.56×10^{21}	30.6	29.1	52.6	50.2	0.52	0.48
700 nm	10^{23}	10^{22}	4.12×10^{21}	2.71×10^{20}	16.4	14.6	40.1	38.4	0.10	0.09

Table 3 Comparison of the suggested photosensor with the existing photosensors

SI. No	Parameters	Step shape double gate photosensor (this work)		Ge-source photo sensor [11]	HG-photosensor [11]
		Ge	Si		
1	Responsivity	0.71	0.68	0.14	0.56
2	Sensitivity	86.2	80.4	68.2	77.5
3	SNR (dB)	72.5	70.2	39	68

4 Conclusion

This study illustrates the application of SSDG-TFET based as photodetector for two different source materials like Si and Ge in the visible range of spectrum. The results show that at shorter wavelength improved optical features are obtained for both the devices. The Ge-GO-SSDG-TFET has enhanced optical figure of merits than Si-GO-SSDG-TFET for wide variation in λ. Results reveal that Ge based photosensor has S_n value of 86.2, responsivity of 71% A/Watt, and SNR of 72.5 dB at λ = 300 nm. Moreover, Ge-GO-SSDG-TFET possess improved electron density and lower tunnel width than conventional Si device. The comparative study reveals that Ge-GO-SSDG TFET based photosensor has improved optical characteristics than the photo sensors in the existing literatures.

Author Contributions The work and manuscript is written Shreyas Tiwari. The suggestions and grammatical corrections have done by Dr. Rajesh Saha and Dr. Tarun Varma.

Data Availability There is no any other data and material associated with this manuscript.

Declarations

Conflict of interest The authors declare that they have no conflict of interest.

References

1. H. Kao, A.S. Verhulst, W.G. Vandenberghe, B. Sorée, G. Groeseneken, K.D. Meyer, Direct and indirect band-to-band tunneling in germanium-based TFETs. IEEE Trans. Electron Devices **59**, 292–301 (2012)
2. B. Fahs et al., Design and modeling of blue-enhanced and bandwidth-extended PN photodiode in standard CMOS technology. IEEE Trans. Electron Devices **64**(7), 2859–2866 (2017). https://doi.org/10.1109/TED.2017.2700389
3. V. Kumari, M. Gupta, M. Saxena, TCAD-based investigation of double gate junctionless transistor for UV photodetector. IEEE Trans. Electron Devices **68**(6), 2841–2847 (2021). https://doi.org/10.1109/TED.2021.3075654
4. Y. Khatami, K. Banerjee, Steep subthreshold slope n- and p-type tunnel-FET devices for low-power and energy-efficient digital circuits. IEEE Trans. Electron Devices **56**(11), 2752–2761 (2009). https://doi.org/10.1109/TED.2009.2030831
5. W.Y. Choi, B.G. Park, J.D. Lee, T.J.K. Liu, Tunneling field-effect transistors (TFETs) with subthreshold swing (SS) less than 60 mV/dec. IEEE Electron Device Lett. **28**(8), 743–745 (2007). https://doi.org/10.1109/LED.2007.901273
6. S.W. Kim, J.H. Kim, T.J. King Liu, W.Y. Choi, B.G. Park, Demonstration of Lshaped tunnel field-effect transistors. IEEE Trans. Electron Devices **63**(4), 1774–1778 (2016). https://doi.org/10.1109/TED.2015.2472496
7. S. Tiwari, R. Saha, Methods to reduce ambipolar current of various TFET structures: a review. SILICON **14**, 6507–6515 (2022). https://doi.org/10.1007/s12633-021-01458-w
8. D.B. Abdi, M. Jagadesh Kumar, Controlling ambipolar current in tunneling FETs using overlapping gate-on-drain. IEEE J. Electron Devices Soc. **2**(6), 187–190 (2014). https://doi.org/10.1109/JEDS.2014.2327626
9. A.K. Singh, M.R. Tripathy, K. Baral, S. Jit, "Design and performance assessment of HfO_2/SiO_2 gate stacked Ge/Si heterojunction TFET on SELBOX substrate (GSHJ-STFET). SILICON **14**(17), 11847–11858 (2022). https://doi.org/10.1007/s12633-022-01898-y
10. R.M. Imenabadi, M. Saremi, W.G. Vandenberghe, A novel PNPN-like Z-shaped tunnel field-effect transistor with improved ambipolar behavior and RF performance. IEEE Trans. Electron Devices **64**(11), 4752–4758 (2017). https://doi.org/10.1109/TED.2017.2755507
11. S. Tiwari, R. Saha, Improved optical performance in near visible light detection photosensor based on TFET. Microelectron. J. **129**, 105554 (2022). https://doi.org/10.1016/j.mejo.2022.105554
12. Y. Wang, C. Li, O. Li, S. Cheng, W. Liu, H. You, Simulation study of dual metal-gate inverted T-shaped TFET for label-free biosensing. IEEE Sens. J. **22**(19), 18266–18272 (2022). https://doi.org/10.1109/JSEN.2022.3195180
13. D. Som, B. Majumdar, S. Kundu, S. Kanungo, Investigation of charge plasma-enhanced tunnel field-effect transistor for hydrogen gas sensing application. IEEE Sens. Lett. **4**(6), 1–4 (2020). https://doi.org/10.1109/LSENS.2020.2988589

14. J. Núñez, M.J. Avedillo, Reducing the impact of reverse currents in tunnel FET rectifiers for energy harvesting applications. IEEE J. Electron Devices Soc. **5**(6), 530–534 (2017). https://doi.org/10.1109/JEDS.2017.2737598
15. S. Tiwari, R. Saha, DC and RF/analog performances of split source horizontal pocket and hetero stack TFETs considering interface trap charges: a simulation study. Microelectron. Reliab. **137**, 114780 (2022)
16. S. Ghosh, P. Pachal, R. Kumar, S. Kundu, J. Ghosh, S.K. Sarkar, Double gate p-n-p-n TFET with hetero oxide dielectric and high-K spacer engineering. IEEE VLSI DEVICE CIRCUIT AND SYSTEM (VLSI DCS) **2020**, 1–5 (2020). https://doi.org/10.1109/VLSIDCS47293.2020.9179943
17. P. Ghosh, B. Bhowmick, Reduction of the kink effect in a SELBOX tunnel FET and its RF/analog performance. J. Comput. Electron. **18**(4), 1182–1191 (2019)
18. A.K. Singh, M.R. Tripathy, R.K. Upadhyay, S. Jit, Design and Simulation of Triple Material Gate InAs/Si Heterojunction TFET on SEL-BOX Substrates: Temperature Impact Analysis, 2021 IEEE 4th International Conference on Computing, Power and Communication Technologies (GUCON), (Kuala Lumpur, Malaysia, 2021), pp. 1–6, https://doi.org/10.1109/GUCON50781.2021.9573526.
19. M. Liu, Q. Xie, S. Xia, and Z. Wang, A Novel Step-shaped Gate Tunnel FET with Low Ambipolar Current, 2019 2nd International Symposium on Devices, Circuits and Systems (ISDCS), 2019, pp. 1-4, https://doi.org/10.1109/ISDCS.2019.8719250
20. R. Saha, D.K. Panda, R. Goswami, Analysis on electrical parameters including temperature and interface trap charges in gate overlap Ge source step shape double gate TFET. Microelectron. J. **130**, 105629 (2022). https://doi.org/10.1016/j.mejo.2022.105629
21. TCAD sentaurus device user guide, synopsys, Inc., (2022)
22. K. Kao, A.S. Verhulst, W.G. Vandenberghe, B. Soree, G. Groeseneken, K.D. Meyer, Direct and indirect band-to-band tunneling in germanium-based TFETs. IEEE Trans. Electron Devices **59**(2), 292–301 (2012). https://doi.org/10.1109/TED.2011.2175228
23. S.H. Kim, H. Kam, C Hu, T.-J.K. Liu, e-source tunnel field effect transistors with record high I_{ON}/I_{OFF}, VLSI Symp. Tech. Dig., pp.178–179, (2009)
24. H. Ferhati, F. Djeffal, L.B. Drissi, Performance assessment of a new infrared phototransistor based on JL-TFET structure: Numerical study and circuit level investigation. Optik, vol. 223, (2020), https://doi.org/10.1016/j.ijleo. 2020.165471
25. R. Paschotta, Optical Heterodyne detection Encyclopedia of Laser Physics and Technology, ed.1 October 2008, ISBN 978- 3–527–40828–3
26. C. Wang et al., High-performance Ge p-n photodiode achieved with preannealing and excimer laser annealing. IEEE Photonics Technol. Lett. **27**(14), 1485–1488 (2015). https://doi.org/10.1109/LPT.2015.2426016.10
27. V.D. Wangkheirakpam, B. Bhowmick, P.D. Pukhrambam, Modeling and simulation of optically gated TFET for near infra-red sensing applications and its low frequency noise analysis. IEEE Sens. J. **20**(17), 9787–9795 (2020). https://doi.org/10.1109/JSEN.2020.2991406
28. S. Joshi, P.K. Dubey, B.K. Kaushik, Photosensor based on split gate TMD TFET using photogating effect for visible light detection. IEEE Sens. J. **20**(12), 6346–6353 (2020). https://doi.org/10.1109/JSEN.2020.2966728

Publisher's Note Springer Nature remains neutral with regard to jurisdictional claims in published maps and institutional affiliations.

Springer Nature or its licensor (e.g. a society or other partner) holds exclusive rights to this article under a publishing agreement with the author(s) or other rightsholder(s); author self-archiving of the accepted manuscript version of this article is solely governed by the terms of such publishing agreement and applicable law.